Reaction of Organic Peroxyl Radicals with ·NO2 and ·NO in Aqueous Solution: Intermediacy of Organic Peroxynitrate and Peroxynitrite Species

3 AUTHORS, INCLUDING:

Sara Goldstein
Hebrew University of Jerusalem
151 PUBLICATIONS 5,956 CITATIONS

Gábor Merényi
KTH Royal Institute of Technology
80 PUBLICATIONS 3,081 CITATIONS

Reaction of Organic Peroxyl Radicals with •NO₂ and •NO in Aqueous Solution: Intermediacy of Organic Peroxynitrate and Peroxynitrite Species

Sara Goldstein,*,† Johan Lind,‡ and Gabor Merenyi‡

Department of Physical Chemistry, The Hebrew University of Jerusalem, Jerusalem 91904, Israel, and Department of Chemistry, Nuclear Chemistry, The Royal Institute of Technology, S-10044 Stockholm 70, Sweden

In this work, we studied the reactions of alkyl peroxyl radicals with •NO₂ and •NO using the pulse radiolysis technique. The rate constants for the reaction of •NO₂ with $(CH_3)_2C(OH)CH_2OO^•$, $CH_3OO^•$, and $c\text{-}C_5H_9OO^•$ vary between 7×10^8 and 1.5×10^9 M^{-1} s^{-1}. The reaction produces relatively long-lived alkyl peroxynitrates, which are in equilibrium with the parent radicals and have no appreciable absorption above 270 nm. It is also shown that •NO adds rapidly to $(CH_3)_2C(OH)CH_2OO^•$ and $CH_3OO^•$ to form alkyl peroxynitrites. The rate constants for these reactions were determined to be 2.8×10^9 and 3.5×10^9 M^{-1} s^{-1}, respectively. However, in contrast to alkyl peroxynitrates, alkyl peroxynitrites do not accumulate. Rather, they decompose rapidly via homolysis along the relatively weak O–O bond, initially forming a geminate pair. Most of this pair collapses in the cage to form an alkyl nitrate, $RONO_2$, and about 14% diffuses out as free alkoxyl and •NO₂ radicals. A thermokinetic analysis predicts the half-life of CH_3OONO in water to be less than 1 μs, an estimate that agrees well with previous experimental findings of ours for other alkyl peroxynitrites. A comparison of aqueous and gaseous thermochemistry of alkyl peroxynitrates reveals that alkyl peroxyl radicals and the corresponding alkyl peroxynitrates are similarly solvated by water.

Introduction

Organic peroxyl radicals, ROO•, are important reactive intermediates in biological and environmental systems; therefore, their reactions with •NO and •NO₂ are potentially of great importance. Indeed, the reaction of •NO with lipid peroxyl radicals has been proposed to account for the inhibitory effect of •NO during lipid peroxidation,[1–6] but the mechanism of these reactions has not yet been fully explained. At present, the inhibition is believed to be contingent on the chain-breaking activity of •NO (i.e., the scavenging of peroxyl and alkoxyl radicals by •NO[1–6]). Nevertheless, not even the mechanism of •NO reacting with simple alcohol-derived peroxyl radicals is fully understood in aqueous solutions.[7] The rate constants for the reaction of •NO with these alkyl peroxyl radicals were determined to be $(1-3) \times 10^9$ M^{-1} s^{-1} by laser-flash photolysis, and it has been proposed that this reaction forms relatively long-lived alkyl peroxynitrites, ROONO, which have maximum absorption around 300 nm.[7] However, such a suggestion does not agree with (i) the tendency of ROONO to homolyze fast along the weak O–O bond forming RO• and •NO₂ radicals;[8] (ii) the fact that HOONO has no appreciable absorption above 280 nm,[9] and it is unlikely that ROONO has a maximum absorption at 300 nm, or even absorbs at all at this region; and (iii) the fact that RO• is known to be unstable toward monomolecular rearrangements, undergoing β scissions[10–12] or a 1,2-H shift when the alkoxyl radical bears α-hydrogen atoms.[13,14] The latter process converts an alkoxyl radical into a α-hydroxy alkyl radical, which reacts rapidly with O₂ to form

$O_2^{•−}$.[15–17] The superoxide radical reacts quickly with •NO and •NO₂ to produce $ONOO^−$ and $O_2NOO^−$, respectively, and these ions have maximum absorption around 300 nm.[9,18–21]

If ROONO homolyzes along the O–O bond forming RO• and •NO₂ radicals, then the reactions of •NO₂ with ROO• and RO• may also take place. However, these reactions have not yet been studied directly in aqueous solution. There is a clear need for a better understanding of the reactions of organic peroxyl radicals with •NO and •NO₂ under physiological conditions. In this paper, we report the results of a pulse radiolysis study of the reactions •NO₂ and •NO with relatively simple alkyl peroxyl radicals such as $CH_3OO^•$, $(CH_3)_2C(OH)CH_2$-$OO^•$, and $c\text{-}C_5H_9OO^•$. Our results show that these peroxyl radicals readily react with •NO₂ and •NO to form alkyl peroxynitrates and peroxynitrites, respectively. We have also demonstrated that alkyl peroxynitrates are relatively stable species, whereas alkyl peroxynitrites rapidly decompose via homolysis along the weak O–O bond.

Experimental Section

Chemicals. All chemicals were of analytical grade and were used as received. Solutions were prepared with distilled water, which was further purified using a Milli-Q water purification system. Tetranitromethane (TNM) is stable in neutral and acidic solutions but hydrolyzes in basic solutions to form about 62% $C(NO_2)_3^-$ ($\epsilon_{350} = 14\,400$ M^{-1} s^{-1}).[22,23] Therefore, the concentration of TNM was determined by measuring its conversion to $C(NO_2)_3^-$ at pH 13. Aqueous solutions saturated with cyclopentane (2.5 mM) were prepared by adding cyclopentane in excess and were vigorously stirred for at least 30 min.

Apparatus. Pulse radiolysis experiments were carried out in Jerusalem with a Varian 7715 linear accelerator with 5-MeV electron pulses of $0.2-1.5$ μs and 200 mA. All measurements

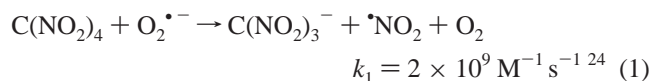* To whom all correspondence should be directed. E-mail: sarag@vms.huji.ac.il.
† The Hebrew University of Jerusalem.
‡ The Royal Institute of Technology.

were made at ambient temperature in a 4-cm Spectrosil cell using three light passes (optical path length 12.1 cm). Each measurement was repeated at least five times. Appropriate cutoff filters were used to eliminate photolysis. Dosimetry was performed with oxygenated solution containing 5 mM ferrocyanide using $G(Fe(CN)_6^{3-})) = 2.7 \times 10^{-7}$ M Gy^{-1} and $\epsilon_{420}(Fe(CN)_6^{3-}) = 1000$ M^{-1} cm^{-1}.

The experimental results were modeled by means of INTKIN, a noncommercial program developed at Brookhaven National Laboratories by Dr. H. A. Schwarz.
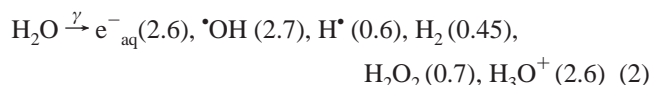
Determination of $O_2^{\bullet-}$. The yield of $O_2^{\bullet-}$ was determined using TNM, which is readily reduced by $O_2^{\bullet-}$ to form $^{\bullet}NO_2$ and the highly absorbing $C(NO_2)_3^{-}$.

$$C(NO_2)_4 + O_2^{\bullet-} \rightarrow C(NO_2)_3^{-} + {}^{\bullet}NO_2 + O_2$$
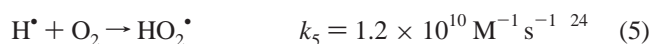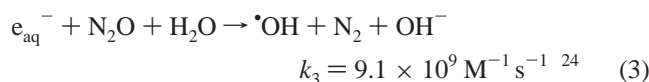$$k_1 = 2 \times 10^9 \text{ M}^{-1}\text{s}^{-1}\ ^{24} \quad (1)$$

The formation of the nitroform ion was followed at 350 nm ($\epsilon_{350} = 14\,400$ M^{-1} s^{-1}) or at 380 nm ($\epsilon_{380} = 4800$ M^{-1} s^{-1}).

Results

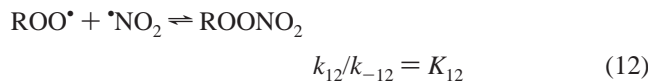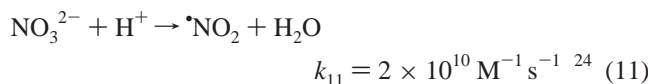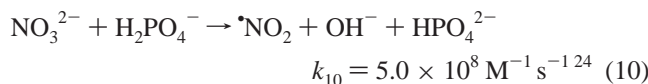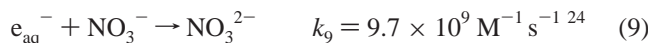**Formation of ROO$^{\bullet}$.** The alkyl peroxyl radical species were generated upon irradiation of aqueous solutions saturated with a 4:1 (v/v) mixture of N$_2$O and O$_2$, which contained the organic compound RH, 5 μM diethylenetriaminepentaacetic acid (DTPA), and 8 mM phosphate buffer (PB). DTPA was added to avoid catalysis by traces of metal impurities of $O_2^{\bullet-}$ decomposition, given that some $O_2^{\bullet-}$ does form in the present system (see below).

$$H_2O \xrightarrow{\gamma} e^-_{aq}(2.6), {}^{\bullet}OH\ (2.7), H^{\bullet}\ (0.6), H_2\ (0.45),$$
$$H_2O_2\ (0.7), H_3O^+\ (2.6) \quad (2)$$

The numbers in parentheses are G values, which represent the concentrations of the species (in 10^{-7} M Gy^{-1}) and are about 7% higher in the presence of high solute concentrations.

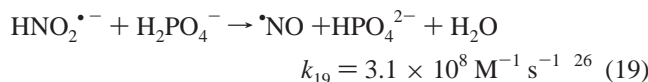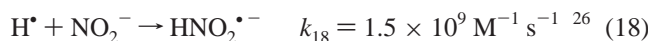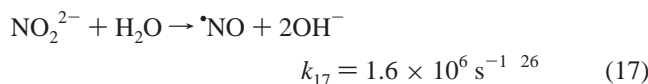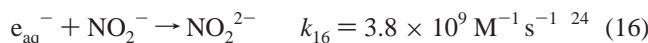$$e^-_{aq} + N_2O + H_2O \rightarrow {}^{\bullet}OH + N_2 + OH^-$$
$$k_3 = 9.1 \times 10^9 \text{ M}^{-1}\text{s}^{-1}\ ^{24} \quad (3)$$

$${}^{\bullet}OH + RH \rightarrow R^{\bullet} + H_2O \quad (4)$$

$$H^{\bullet} + O_2 \rightarrow HO_2^{\bullet} \quad k_5 = 1.2 \times 10^{10} \text{ M}^{-1}\text{s}^{-1}\ ^{24} \quad (5)$$

$$HO_2^{\bullet} \rightleftharpoons H^+ + O_2^{\bullet-} \quad pK_a = 4.8\ ^{25} \quad (6)$$

$$R^{\bullet} + O_2 \rightarrow ROO^{\bullet} \quad (7)$$

$$ROO^{\bullet} + ROO^{\bullet} \rightarrow xO_2^{\bullet-} + \text{products} \quad (8)$$

Formation of ROO$^{\bullet}$ and $^{\bullet}NO_2$. ROO$^{\bullet}$ and $^{\bullet}NO_2$ are generated in approximately equal amounts upon irradiation of aerated aqueous solutions containing excess of RH over NO$_3^-$, 5 μM DTPA, and a buffer. Under these conditions, $^{\bullet}$OH is converted to ROO$^{\bullet}$ (reactions 4 and 7), and e^-_{aq} is converted to $^{\bullet}NO_2$ radicals (reactions 9–11). The latter reacts readily with ROO$^{\bullet}$ (reaction 12) and $O_2^{\bullet-}$ (reaction 13).

$$e^-_{aq} + NO_3^- \rightarrow NO_3^{2-} \quad k_9 = 9.7 \times 10^9 \text{ M}^{-1}\text{s}^{-1}\ ^{24} \quad (9)$$

$$NO_3^{2-} + H_2PO_4^- \rightarrow {}^{\bullet}NO_2 + OH^- + HPO_4^{2-}$$
$$k_{10} = 5.0 \times 10^8 \text{ M}^{-1}\text{s}^{-1}\ ^{24} \quad (10)$$

$$NO_3^{2-} + H^+ \rightarrow {}^{\bullet}NO_2 + H_2O$$
$$k_{11} = 2 \times 10^{10} \text{ M}^{-1}\text{s}^{-1}\ ^{24} \quad (11)$$

$$ROO^{\bullet} + {}^{\bullet}NO_2 \rightleftharpoons ROONO_2$$
$$k_{12}/k_{-12} = K_{12} \quad (12)$$

$${}^{\bullet}NO_2 + O_2^{\bullet-} \rightleftharpoons O_2NO_2^-$$
$$k_{13} = 4.5 \times 10^9 \text{ M}^{-1}\text{s}^{-1}\ ^{18}$$
$$k_{-13} = 1.3 \text{ s}^{-1}\ ^{21} \quad (13)$$

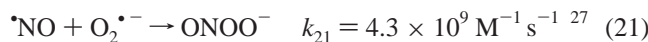$$O_2NO_2^- \rightarrow NO_2^- + O_2 \quad k_{14} = 1.1 \text{ s}^{-1}\ ^{21} \quad (14)$$
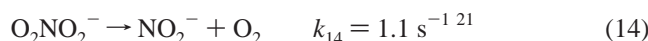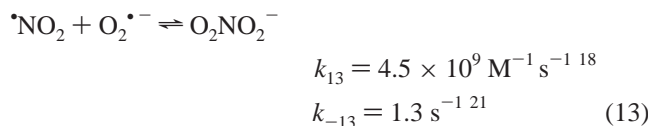
Under such conditions, ROO$^{\bullet}$ is consumed via reactions 8 and 12, and the rate equation (eq 15) is given for its decay:

$$-\frac{d[ROO^{\bullet}]}{dt} = 2k_8[ROO^{\bullet}]^2 + k_{12}[ROO^{\bullet}][{}^{\bullet}NO_2] \quad (15)$$

Formation of ROO$^{\bullet}$ and $^{\bullet}NO$. Approximately equal amounts of ROO$^{\bullet}$ and $^{\bullet}NO$ are generated when NO$_3^-$ is replaced by NO$_2^-$ and e^-_{aq} and H$^{\bullet}$ are converted to $^{\bullet}NO$ (reactions 16–19).

$$e^-_{aq} + NO_2^- \rightarrow NO_2^{2-} \quad k_{16} = 3.8 \times 10^9 \text{ M}^{-1}\text{s}^{-1}\ ^{24} \quad (16)$$

$$NO_2^{2-} + H_2O \rightarrow {}^{\bullet}NO + 2OH^-$$
$$k_{17} = 1.6 \times 10^6 \text{ s}^{-1}\ ^{26} \quad (17)$$

$$H^{\bullet} + NO_2^- \rightarrow HNO_2^{\bullet-} \quad k_{18} = 1.5 \times 10^9 \text{ M}^{-1}\text{s}^{-1}\ ^{26} \quad (18)$$

$$HNO_2^{\bullet-} + H_2PO_4^- \rightarrow {}^{\bullet}NO + HPO_4^{2-} + H_2O$$
$$k_{19} = 3.1 \times 10^8 \text{ M}^{-1}\text{s}^{-1}\ ^{26} \quad (19)$$

Under such conditions, $^{\bullet}NO$ readily reacts with ROO$^{\bullet}$ and $O_2^{\bullet-}$:

$$ROO^{\bullet} + {}^{\bullet}NO \rightarrow \text{products} \quad (20)$$

$${}^{\bullet}NO + O_2^{\bullet-} \rightarrow ONOO^- \quad k_{21} = 4.3 \times 10^9 \text{ M}^{-1}\text{s}^{-1}\ ^{27} \quad (21)$$

Hence, ROO$^{\bullet}$ decays via reactions 8 and 20 and the rate equation (eq 15a) is obtained for its decay:

$$-\frac{d[ROO^{\bullet}]}{dt} = 2k_8[ROO^{\bullet}]^2 + k_{20}[ROO^{\bullet}][{}^{\bullet}NO] \quad (15a)$$

In cases where the rate of the self-decay of ROO$^{\bullet}$ cannot be ignored, we corrected for the contribution of this process by computer modeling, as will be described below. Consequently, an accurate value of k_8 is required for the determination of both k_{12} and k_{20}.

Self-Decomposition of ROO$^{\bullet}$. The rate constant for the self-decomposition of CH$_3$OO$^{\bullet}$ has recently been redetermined to be $2k_8 = (7.3 \pm 1.9) \times 10^8$ M^{-1} s^{-1},[8] and the yield of $O_2^{\bullet-}$ formed in this process was found to be $29 \pm 3\%$ (i.e., $x = 0.58$).[8] The literature values of $2k_8$ for the self-decomposition of c-C$_5$H$_9$OO$^{\bullet}$ vary between 1.5×10^7 M^{-1} s^{-1} [28] and 2.4×10^7 M^{-1} s^{-1},[29] and c-C$_5$H$_9$OO$^{\bullet}$ was shown not to produce $O_2^{\bullet-}$ during its decomposition.[29] The rate constant for the self-

decomposition of $(CH_3)_2C(OH)CH_2OO^\bullet$ varies in the literature between $2k_8 = 1.8 \times 10^8$ M^{-1} s^{-1} [30] and 8×10^8 M^{-1} s^{-1}.[31] These values are significantly higher than those reported for c-$C_5H_9OO^\bullet$; therefore, it was essential to redetermine $2k_8$ for $(CH_3)_2C(OH)CH_2OO^\bullet$.

$(CH_3)_2C(OH)CH_2OO^\bullet$ was generated upon irradiation (14 Gy/pulse) of aqueous solutions saturated with N_2O/O_2 (4:1), which contained 0.1–0.5 M *tert*-butanol, 5 μM DTPA, and 4–10 mM PB at pH 5.0–9.8. The absorption formed immediately after the pulse is the sum of $(CH_3)_2C(OH)CH_2OO^\bullet$ (G = 5.7) and $O_2^{\bullet-}$ (G = 0.6), and the extinction coefficients of $(CH_3)_2C(OH)CH_2OO^\bullet$ were calculated using the well-established spectrum of $O_2^{\bullet-}$ [25] (e.g., $\epsilon_{260} = 1050 \pm 100$ M^{-1} cm^{-1}, $\epsilon_{280} = 890 \pm 60$ M^{-1} cm^{-1}). The absorption decayed via two sequential second-order reactions. The first second-order decay, which was hardly affected at all by [*tert*-butanol] or the pH, was attributed to reaction 8, where $2k_8 = (8 \pm 2) \times 10^8$ M^{-1} s^{-1}. This value is similar to that previously determined at pH 9.4 using conductivity detection.[31] The rate of the second decay decreased with increasing pH and is attributed to the dismutation of $O_2^{\bullet-}$, which is formed by the pulse and during the decomposition of the peroxyl radical.[31] The yield of $O_2^{\bullet-}$ thus formed was determined after the addition of 100 μM TNM (reaction 1), which is sufficient to compete efficiently with the dismutation of $O_2^{\bullet-}$ and with its reaction with •NO₂. The fast formation of $C(NO_2)_3^-$, which was complete within less than 100 ms, was followed by a slower formation reaction. We attribute the first process to reduction by the $O_2^{\bullet-}$ formed by the pulse, $[O_2^{\bullet-}]_o$, and during the self-decomposition of $(CH_3)_2C(OH)CH_2OO^\bullet$. We also measured the total yield of the nitroform ion, $\Delta[C(NO_2)_3^-]_F$, produced in this process. The yield of $O_2^{\bullet-}$ formed during the self-decomposition of $(CH_3)_2C(OH)CH_2OO^\bullet$ was calculated according to eq 22 to be $27 \pm 3\%$. The latter value is somewhat higher than the one determined previously using conductivity detection (i.e., 19%[31]).

$$\text{yield}(O_2^{\bullet-})_F = \frac{\Delta[C(NO_2)_3^-]_F - [O_2^{\bullet-}]_o}{[ROO^\bullet]_o - \Delta[C(NO_2)_3^-]_F} \quad (22)$$

The reduction of TNM by $O_2^{\bullet-}$ yields $C(NO_2)_3^-$ and •NO₂, and •NO₂ is expected to react rapidly with $(CH_3)_2C(OH)CH_2OO^\bullet$. We therefore suggest the second and slow generation of $C(NO_2)_3^-$, whose yield is $\Delta[C(NO_2)_3^-]_S$, to be due to $O_2^{\bullet-}$ formed during the decomposition of $(CH_3)_2C(OH)CH_2OONO_2$. For this reason, $[(CH_3)_2C(OH)CH_2OONO_2] = \Delta[C(NO_2)_3^-]_F$, and the yield of $O_2^{\bullet-}$ formed during the decomposition of $(CH_3)_2C(OH)CH_2OONO_2$ was calculated according to eq 23 to be $24 \pm 5\%$.

$$\text{yield}(O_2^{\bullet-})_S = \frac{\Delta[C(NO_2)_3^-]_S}{\Delta[C(NO_2)_3^-]_F} \quad (23)$$

Our results show that the yield of $O_2^{\bullet-}$ formed during the self-

SCHEME 1

$$ROONO_2 \underset{k_{12}}{\overset{k_{-12}}{\rightleftharpoons}} ROO^\bullet + {}^\bullet NO_2 \qquad (-12)$$

$$ROO^\bullet + ROO^\bullet \xrightarrow{k_8} xO_2^{\bullet-} + \text{products} \qquad (8)$$

$$2\,{}^\bullet NO_2 + H_2O \xrightarrow{k_{24}} NO_3^- + NO_2^- + 2H^+ \qquad 2k_{24} = 1.3 \times 10^8 \text{ M}^{-1}\text{s}^{-1}\,{}^{24} \quad (24)$$
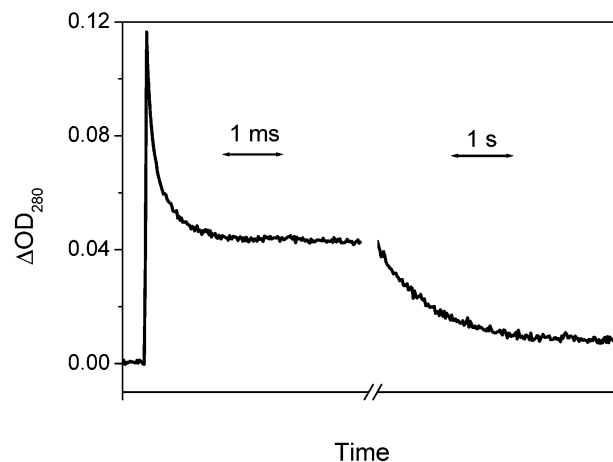

Figure 1. Formation and decay of the absorption at 280 nm observed after pulse irradiation (35 Gy/pulse) of an aerated solution containing 0.1 M *tert*-butanol, 5 mM nitrate, 5 μM DTPA, and 8 mM PB at pH 7.1. The optical path length was 12.1 cm.

decomposition of $(CH_3)_2C(OH)CH_2OO^\bullet$ is, within experimental error, the same as that produced during the decomposition of $(CH_3)_2C(OH)CH_2OONO_2$. We therefore suggest that the decomposition of $(CH_3)_2C(OH)CH_2OONO_2$ is similar to that of $HOONO_2$[18,20,21] (i.e., $ROONO_2$ decomposes via reactions −12, 12, 8, and 24; Scheme 1).

Reaction of ROO• with •NO₂. Approximately equal amounts of ROO• and •NO₂ were generated upon irradiation (14–38 Gy/pulse) of aerated solutions containing RH (0.02–0.3 M DMSO, 0.1–1 M *tert*-butanol, or 2.5 mM cyclopentane), 5 mM NO_3^-, 5 μM DTPA, and 8 mM PB. The reaction could be studied at a concentration level of 2.5 mM cyclopentane because •OH reacts with cyclopentane ca. 100 times faster than with NO_3^-.[24] In all three cases, the absorption at 250–300 nm decayed via a fast second-order reaction, which was followed by a first-order process. Typical kinetic traces at pH 7.1 are shown in Figure 1 for *tert*-butanol. The rate of the fast second-order process was independent of the pH (3.6–7.7), pulse intensity, and [RH]; therefore, it was attributed to the decay of ROO• via reactions 8 and 12. In the case of c-$C_5H_9OO^\bullet$, the experimental second-order rate constant for the decay of the absorption at 270 nm was $k/\epsilon l = (1.1 \pm 0.1) \times 10^5$ s^{-1} compared to 450 ± 100 s^{-1} in the absence of •NO₂. Therefore, the measured value was converted to $k_{12} = (1.5 \pm 0.2) \times 10^9$ M^{-1} s^{-1} using ϵ_{270}(c-$C_5H_9OO^\bullet$) = 1100 ± 100 M^{-1} cm^{-1} and $l = 12.1$ cm. In the DMSO and *tert*-butanol systems, the experimental observed second-order rate constants for the decay of the absorption at 280 nm were $k/\epsilon l = (2.2 \pm 0.2) \times 10^5$ and $(1.5 \pm 0.1) \times 10^5$ s^{-1}, respectively. In these two systems, the contribution of reaction 8 cannot be ignored; therefore, we have resorted to computer modeling using reactions 8, 12, 13, and 24 (Figure 2). The derived k_{12} values are 7×10^8 M^{-1} s^{-1} and 1×10^9
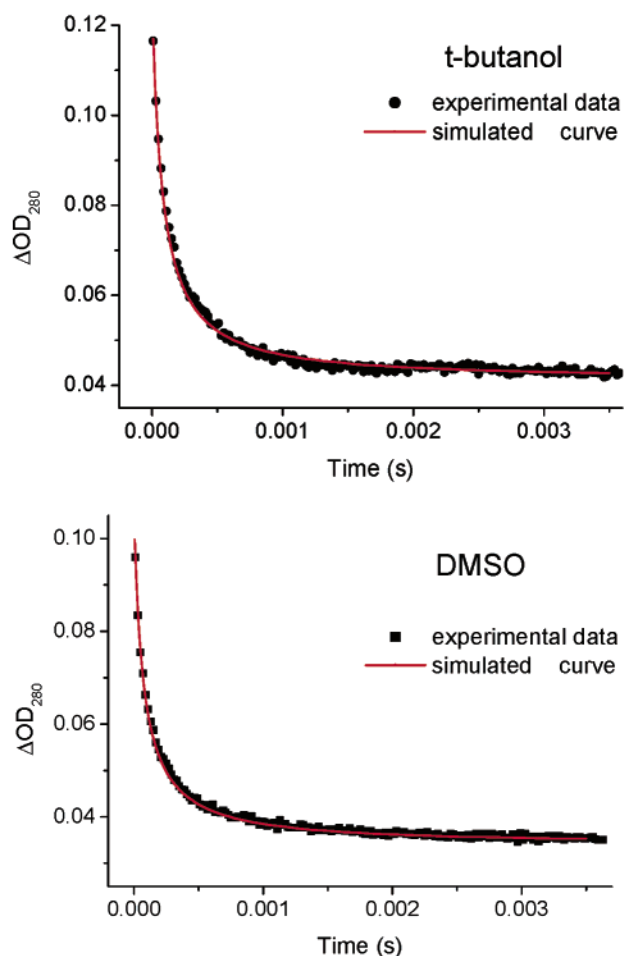
Figure 2. Simulated and observed curves for the fast decay of the absorbance at 280 nm obtained after pulse irradiation of an aerated solution containing 5 mM nitrate, 5 μM DTPA, 8 mM PB (pH 7.1), and 0.1 M *tert*-butanol (35 Gy/pulse) or 20 mM DMSO (31.5 Gy/pulse). The time course was simulated using reactions 8, 12, 13, and 24, $\epsilon((CH_3)_2C(OH)CH_2OO^\bullet) = 890$ M^{-1} cm^{-1}, $\epsilon(CH_3OO^\bullet) = 850$ M^{-1} cm^{-1}, $k_{13} = 4.5 \times 10^9$ M^{-1} s^{-1}, $2k_{24} = 1.3 \times 10^8$ M^{-1} s^{-1}, and $\epsilon(O_2^{\bullet-}) = 900$ M^{-1} cm^{-1}. The best fit was obtained using $2k_8 = 8 \times 10^8$ M^{-1} s^{-1}, $x = 0.25$, $\epsilon(O_2NOO^-) = 1200$ M^{-1} cm^{-1}, and $k_{12} = 7 \times 10^8$ M^{-1} s^{-1} for *tert*-butanol or 1×10^9 M^{-1} s^{-1} for DMSO.

M^{-1} s^{-1} in the *tert*-butanol and DMSO systems, respectively. All of the determined rate constants are summarized in Table 1.

The observed first-order rate constant for the second process was determined to be 1.3 ± 0.2 s^{-1} at pH 7.1 and 7.7 and 0.42 ± 0.03 s^{-1} at pH 6.0. Also, the contribution of the second decay decreased upon decreasing the wavelength and/or the pH. Therefore, the second process is attributed to the decomposition of O$_2$NOO$^-$ because it has a maximum absorption at 285 nm
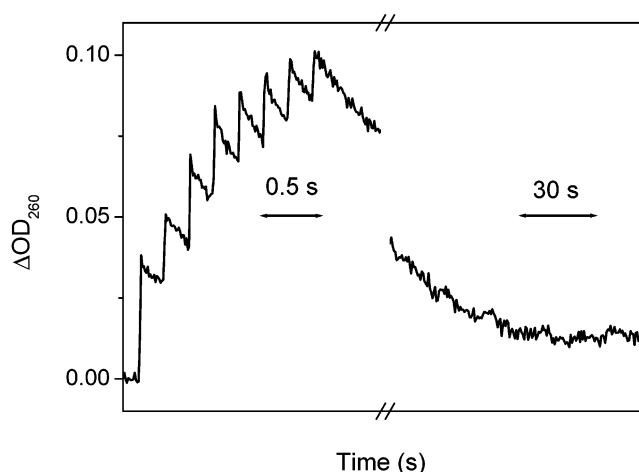

Figure 3. Decay of the absorption at 260 nm after eight repetitive pulsings (38 Gy/pulse) of an aerated solution containing 0.02 M DMSO, 3 mM nitrate, 5 μM DTPA, and 8 mM PB at pH 7.1. The optical path length was 12.1 cm.

($\epsilon_{285} = 1500 \pm 100$ M^{-1} cm^{-1}) and a half-life of about 0.5 s at 25 °C, whereas O$_2$NOOH (p$K_a = 5.9$) is a relatively long-lived species with no appreciable absorption at $\lambda > 260$ nm.[18,20,21]

A residual absorption was observed in all cases, which increased with decreasing wavelength and decayed very slowly to zero. In the case of c-C$_5$H$_9$OO$^\bullet$, this third decay obeyed first-order kinetics, and k_{obs} was measured to be 0.026 ± 0.006 s^{-1}. The residual absorptions in the cases of CH$_3$OO$^\bullet$ and (CH$_3$)$_2$C-(OH)CH$_2$OO$^\bullet$ were relatively small; therefore, we used repetitive pulsing to achieve higher concentrations of the absorbing species. As seen in Figure 3, the delay between the pulses was sufficient for the complete decomposition of ROO$^\bullet$ but not of O$_2$NOO$^-$, which is also accumulated in this system. The third decay process, which is well separated from the decay of O$_2$NOO$^-$, obeyed first-order kinetics and for both radicals k_{obs} was measured to be 0.038 ± 0.012 s^{-1}. This slow first-order reaction is attributed to the decomposition of ROONO$_2$, which absorbs very little in this region, as is also the case with HOONO$_2$.[18] The decomposition of ROONO$_2$ is proposed to take place by way of reactions -12, 12, 8, and 24, where $k_{12} > k_8 > k_{24}$ (Scheme 1). Thus, upon assuming the steady-state approximation for [ROO$^\bullet$] and [$^\bullet$NO$_2$], the rate equation will be given by

$$-\frac{d[ROONO_2]}{dt} = \frac{2k_8 k_{-12}}{2k_8 + k_{12}(k_8/k_{24})^{1/2}}[ROONO_2]$$

$$\approx K_{-12}(2k_8 2k_{24})^{1/2}[ROONO_2] \qquad (25)$$

Thus, $k_{obs} \approx K_{-12}(2k_8 2k_{24})^{1/2}$, and one calculates $K_{-12} \approx 1 \times$

TABLE 1: Summary of the Rate Constants Used and Determined in the Present Study

	CH$_3$	(CH$_3$)$_2$C(OH)CH$_2$	c-C$_5$H$_9$	H
2ROO$^\bullet \rightarrow x$O$_2^{\bullet-}$ + products				
$2k_8$, M^{-1} s^{-1}	$(7.3 \pm 1.6) \times 10^8$	$(8 \pm 2) \times 10^8$	$(1.5-2.4) \times 10^7$	1.7×10^6 [25]
x	0.58	0.54	ca. 0	
ROO$^\bullet$ + $^\bullet$NO$_2$ ⇌ ROONO$_2$				
k_{12}, M^{-1} s^{-1}	1×10^9	7×10^8	$(1.5 \pm 0.2) \times 10^9$	$(1.8 \pm 0.2) \times 10^9$ [18]
k_{-12}, s^{-1}	~0.1	~0.07	~0.75	0.026 ± 0.003 [21]
K_{-12}, M	~1×10^{-10}	~1×10^{-10}	~5×10^{-10}	1.4×10^{-11}
ROO$^\bullet$ + $^\bullet$NO ⇌ ROONO				
k_{20}, M^{-1} s^{-1}	3.5×10^9	2.8×10^9		$(3.2 \pm 0.3) \times 10^9$ [19]
RO$^\bullet$ + $^\bullet$NO$_2$ ⇌ ROONO				
k_{33}, M^{-1} s^{-1}	~1×10^9			$(4.5 \pm 1.0) \times 10^9$ [45]
k_{-33}, s^{-1}	~5×10^5			~1 [45]

Reaction of Peroxyl Radicals with •NO$_2$ and •NO

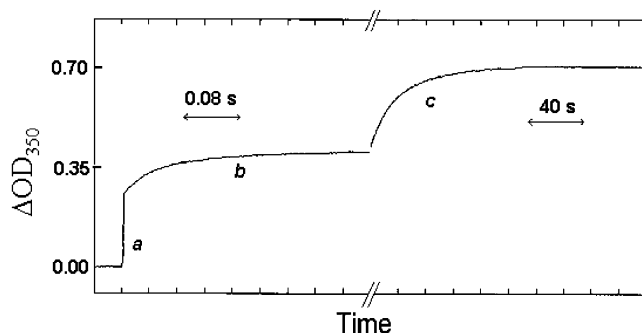*J. Phys. Chem. A, Vol. 108, No. 10, 2004* **1723**

Figure 4. Formation of the absorbance at 350 nm after pulse irradiation (32 Gy/pulse) of an aerated solution containing 0.28 M DMSO, 30 mM nitrate, 5 μM DTPA, 32 μM TNM, and 30 mM PB at pH 7.1. In this system, CH$_3$OO• decomposes via reactions 8 and 20; therefore, O$_2$•$^-$ is formed relatively quickly by the pulse (*a*), through reaction 8 (*b*) and during the slow decomposition of CH$_3$OONO$_2$ (*c*). The optical path length was 12.1 cm.

10^{-10} M for CH$_3$OO• and (CH$_3$)$_2$C(OH)CH$_2$OO• and $K_{-12} \approx 5 \times 10^{-10}$ M for c-C$_5$H$_9$OO•. The equilibrium constant for CH$_3$-OO• is in fair agreement with our earlier indirect determination of $K_{-12} \approx 5 \times 10^{-11}$ M, where methyl peroxynitrate arose after the reaction of ONOO$^-$ with acetone in the presence of TNM.[8]

Our proposed mechanism for the decomposition of ROONO$_2$ involves the formation of O$_2$•$^-$; therefore, one should also be able to determine the rate constant for this process using TNM. This method was tested in the case of CH$_3$OO•, where we studied the reaction of CH$_3$OO• with •NO$_2$ at pH 7.1 in the presence relatively low concentrations of TNM (i.e., 32−65 μM) to minimize photolysis. In this system, CH$_3$OO• decomposes via reactions 8 and 20; therefore, O$_2$•$^-$ is formed relatively quickly by the pulse, through reaction 8 and during the slow decomposition of CH$_3$OONO$_2$. This is seen clearly in Figure 4a−c, respectively. The slow formation of C(NO$_2$)$_3$$^-$ obeyed first-order kinetics, and k_{obs} was measured to be 0.027 ± 0.006 s^{-1}, which agrees with the value obtained directly (see above).

The yield of O$_2$•$^-$, formed via the decomposition of CH$_3$-OONO$_2$, was determined in the absence of NO$_3$$^-$ in solutions saturated with mixtures of 90% N$_2$O and 10% O$_2$. The latter system is less complicated than the former one because CH$_3$-OO• decomposes only via reaction 8 and •NO$_2$ is formed solely through the reduction of TNM by O$_2$•$^-$. Therefore, in this case [CH$_3$OONO$_2$] = Δ[C(NO$_2$)$_3$$^-$]$_F$. Using eqs 22 and 23, we found that the yield of O$_2$•$^-$ formed via reaction 8 is identical to the one formed during the decomposition of CH$_3$OONO$_2$ (i.e., 29 ± 3%). This last result demonstrates again that CH$_3$OONO$_2$ decomposes via reactions −12, 12, 8, and 24 (Scheme 1).

Reaction of ROO• with •NO. •NO and CH$_3$OO• or (CH$_3$)$_2$C(OH)CH$_2$OO• were generated upon irradiation (34 Gy/pulse) of aerated solutions containing 1 M *tert*-butanol or 0.3 M DMSO, 5 mM NO$_2$$^-$, 5 μM DTPA, and 10 mM PB at pH 4.9. The reaction was studied at pH 4.9 to minimize the contributions of peroxynitrite and peroxynitrate to the absorption at 290 nm (i.e., ONOOH (pK_a = 6.6) and O$_2$NOOH (pK_a = 5.9) have no appreciable absorption at this wavelength[9,18]). The
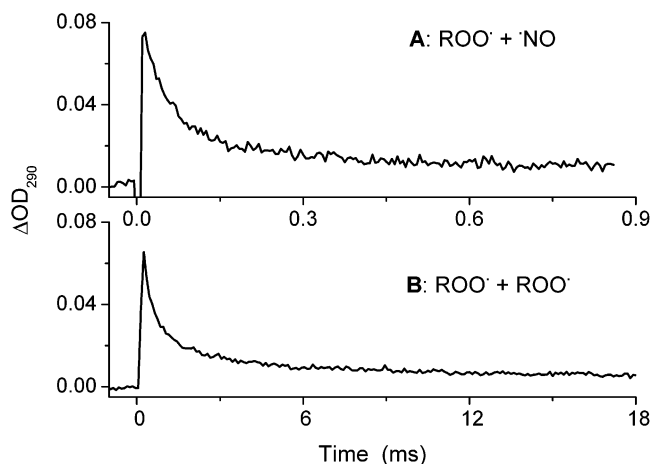

Figure 5. Kinetic traces obtained upon pulse irradiation of (A) an aerated solution containing 0.5 M *tert*-butanol, 5 mM nitrite, 5 μM DTPA, and 10 mM PB at pH 4.9 with 34 Gy/pulse and (B) the same solution saturated with 80% N$_2$O and 20% O$_2$ but without nitrite and with 14 Gy/pulse. The optical path length was 12.1 cm.

reaction could not be studied with 2.5 mM cyclopentane because •OH reacts faster with NO$_2$$^-$ than with cyclopentane.[24] Typical kinetic plots for the decay of (CH$_3$)$_2$C(OH)CH$_2$OO• in the absence and presence of •NO at pH 4.9 are shown in Figure 5. The experimental observed second-order rate constants for the decay of the absorption at 290 nm were $k/\epsilon l$ = (7.2 ± 0.5) × 10^5 and (4.0 ± 0.3) × 10^5 s^{-1} in the DMSO and *tert*-butanol systems, respectively. These rate constants are significantly higher than those measured for the self-decomposition of CH$_3$-OO• and (CH$_3$)$_2$C(OH)CH$_2$OO• (i.e., (5.3 ± 0.5) × 10^4 and (3.2 ± 0.3) × 10^4 s^{-1}, respectively). Therefore, we assume that k_{obs} ≈ 2k_8 + k_{20} (see rate eq 15a), and the k_{20} values were calculated to be (3.7 ± 0.6) × 10^9 and (3.0 ± 0.9) × 10^9 M^{-1} s^{-1} using ϵ_{290}(CH$_3$OO•) = 500 ± 50 M^{-1} cm^{-1} and ϵ_{290}((CH$_3$)$_2$C(OH)CH$_2$-OO•) = 780 ± 80 M^{-1} cm^{-1}, respectively. We corrected the contribution of reaction 8 by computer modeling using reactions 8, 20, and 21 and obtained our best fit for k_{20} = 3.5 × 10^9 and 2.8 × 10^9 M^{-1} s^{-1} for the DMSO and *tert*-butanol systems, respectively. The latter values demonstrate that at least in the initial stage of these reactions k_{obs} ≈ 2k_8 + k_{20}.
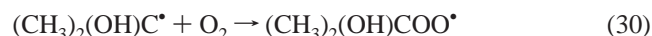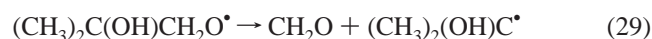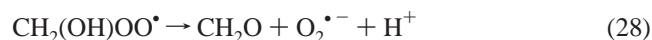
The reactions of •NO with (CH$_3$)$_2$C(OH)CH$_2$OO• and CH$_3$-OO• were investigated in the presence of 55 or 80 μM TNM at pH 6.1−6.9 (34 Gy/pulse). The formation of C(NO$_2$)$_3$$^-$, completed within less than 1 ms, was followed at 380 nm. In these systems, C(NO$_2$)$_3$$^-$ is formed as follows: (i) The solvated electrons react with TNM ca. 10 times faster than with NO$_2$$^-$;[24] therefore, in the presence of 55−80 μM TNM, ca. 10−14%, respectively, of the solvated electrons produce C(NO$_2$)$_3$$^-$ and •NO$_2$; (ii) ROO• decomposes mainly via reactions 8 and 20, where the former reaction forms O$_2$•$^-$; (iii) In aerated solutions containing 5 mM NO$_2$$^-$, ca. 28% of H• forms O$_2$•$^-$ and the rest forms •NO; and (iv) •NO$_2$ and •NO add rapidly to ROO• and O$_2$•$^-$. Altogether, the measured yield of C(NO$_2$)$_3$$^-$ was calculated to be G(C(NO$_2$)$_3$$^-$) ≈ 0.46 or 0.58 in the presence of 55 or 80

SCHEME 2
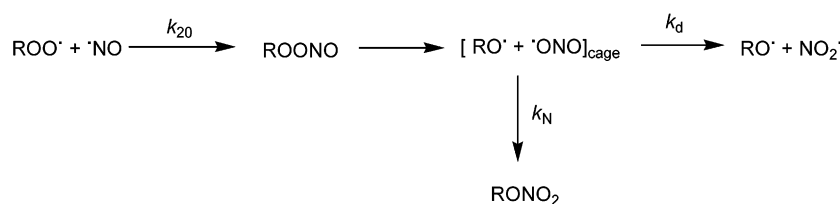
μM TNM, respectively. However, the measured yield was $G(C(NO_2)_3^-) = 0.70 \pm 0.04$ or 0.82 ± 0.06 in the presence of 55 or 80 μM TNM, respectively. These results suggest that $O_2^{\bullet -}$ is also formed via the decomposition of the alkyl peroxynitrites. Our proposed mechanism, which is given in Scheme 2, is similar to the one previously suggested for other alkyl peroxyl radicals.[8]

Alkoxyl radicals $CH_3O^\bullet$ and $(CH_3)_2C(OH)CH_2O^\bullet$ decompose rapidly to give 100% $O_2^{\bullet -}$ via reactions 26–28 or 29–31, respectively.

$$CH_3O^\bullet \rightarrow {}^\bullet CH_2OH \tag{26}$$

$${}^\bullet CH_2OH + O_2 \rightarrow CH_2(OH)OO^\bullet \tag{27}$$

$$CH_2(OH)OO^\bullet \rightarrow CH_2O + O_2^{\bullet -} + H^+ \tag{28}$$

$$(CH_3)_2C(OH)CH_2O^\bullet \rightarrow CH_2O + (CH_3)_2(OH)C^\bullet \tag{29}$$

$$(CH_3)_2(OH)C^\bullet + O_2 \rightarrow (CH_3)_2(OH)COO^\bullet \tag{30}$$

$$(CH_3)_2(OH)COO^\bullet \rightarrow (CH_3)_2CO + O_2^{\bullet -} + H^+ \tag{31}$$

We simulated the yield of $C(NO_2)_3^-$ assuming that ROONO decomposes rapidly according to Scheme 2 and that $RO^\bullet$ yields 100% $O_2^{\bullet -}$. We found for both systems that ROONO decomposes rapidly to form $14 \pm 2\%$ free alkoxyl and $^\bullet NO_2$ radicals.

Discussion

In the present study, we have shown that $ROO^\bullet$ readily reacts with $^\bullet NO_2$ to form relatively long-lived peroxynitrate species, which have no appreciable absorption above 270 nm and are in equilibrium with the parent radicals (Scheme 1). Similar findings were previously described for peroxynitric acid, which decomposes slowly in acidic solutions via equilibrium 12 (where R = H), hydrolysis of $^\bullet NO_2$ (reaction 24), and dismutation of $HO_2^\bullet$ (Table 1).[20,21,32] We have also shown that $CH_3OO^\bullet$ and $(CH_3)_2C(OH)CH_2OO^\bullet$ rapidly react with $^\bullet NO$ to form alkyl peroxynitrites, which do not accumulate but rapidly decompose via homolysis along the O–O bond, initially forming a geminate pair. Most of this pair collapses in the cage to form alkyl nitrates, $RONO_2$, but about 14% diffuses out as free alkoxyl and $^\bullet NO_2$ radicals. The latter value is similar to those recently reported for other alkylperoxynitrites.[8]

In the gas phase, there exists a substantial body of data related to the kinetics of decomposition of alkylperoxynitrates.[33–37] It has been well established that, just as in aqueous solutions, the rate-determining step in the decomposition of a particular $ROONO_2$ is the dissociation to $^\bullet NO_2$ and $ROO^\bullet$. In a few cases, the rates of the reverse reactions are also known,[37] which allows the equilibrium constants to be calculated. A number of important points can be deduced from these data. First, the gaseous rate constants of dissociation, k_{-12}, and their activation energies correlate well with the inductive effect of the substituent and show that the substituent affects the strength of the corresponding O–N bond in the peroxynitrate. The rate constants for the reaction of $ROO^\bullet$ with $^\bullet NO_2$ have values on the order of 10^9 M^{-1} s^{-1} and are insensitive to the substituent. For $C_2H_5OONO_2$, CH_3OONO_2, $HOONO_2$, and CF_3OONO_2, the gaseous equilibrium constants of dissociation, $K_{-12}(g)$, are 1.1×10^{-9}, 6.6×10^{-10}, 1.1×10^{-10}, and 1.3×10^{-11} M, respectively. The increasing stability of the peroxynitrate in the above series reflects the increase in the N–O bond strength, which also parallels the O–H bond strength of the corresponding alkyl hydroperoxide ROOH.[38]

Upon comparing the gaseous and aqueous K_{-12} values of CH_3OONO_2 and $HOONO_2$, we find that their ratio, $K_{-12}(g)/K_{-12}(aq)$, is about the same for both compounds and amounts to a factor of ca. 7. A factor of ca. 4 follows from Henry's constant for $^\bullet NO_2$.[39] This implies that $ROONO_2$ and $ROO^\bullet$ are similarly solvated by water, their Henry's constants differing by less than a factor of 2. Given that the main effect of water is to increase the Gibbs energy of $^\bullet NO_2$, it is not surprising to find that the rate constant of the endergonic reaction (eq -12) is smaller in water than in the gas phase by about an order of magnitude whereas k_{12} is about the same.

To obtain the aqueous Gibbs energies for CH_3OONO_2 and CH_3OONO, we utilize literature data[40] to estimate $\Delta_f G^\circ(CH_3OO^\bullet) \approx 11.3$ kcal/mol and $\Delta_f G^\circ(CH_3O^\bullet) \approx 8$ kcal/mol. Then, by taking $\Delta_f G^\circ(^\bullet NO_2) = 15.1$ kcal/mol[41] and $K_{-12} = 10^{-10}$ M (Table 1) we obtain $\Delta_f G^\circ(CH_3OONO_2) \approx 12.8$ kcal/mol. It is to be expected that the variation in the N–O bond strength with the substituent is similar in peroxynitrates and peroxynitrites. This assumption implies that

$$\Delta_f G^\circ(HOONO) - \Delta_f G^\circ(HOONO_2) \approx$$
$$\Delta_f G^\circ(CH_3OONO) - \Delta_f G^\circ(CH_3OONO_2) \tag{32}$$

Because $\Delta_f G^\circ(HOONO) = 7.1$ kcal/mol[42] and $\Delta_f G^\circ(HOONO_2) = 1.3$ kcal/mol,[32] it follows that $\Delta_f G^\circ(CH_3OONO) \approx 18.6$ kcal/mol. Using the latter value, $\Delta_f G^\circ(^\bullet NO_2) = 15.1$ kcal/mol,[41] and $\Delta_f G^\circ(CH_3O^\bullet) = 8$ kcal/mol, we calculate $K_{33} \approx 2 \times 10^3$ M^{-1}.

$$CH_3O^\bullet + {}^\bullet NO_2 \rightleftharpoons CH_3OONO \tag{33}$$

Because k_{33} is almost certainly close to 10^9 M^{-1} s^{-1},[43] k_{-33} should be $\sim 5 \times 10^5$ s^{-1}, and the overall rate of CH_3OONO disappearance is about 7 times higher (ca. 14% of the radicals escape to the bulk of the solution, i.e., ca. 3.5×10^6 s^{-1}). Indeed, similar values were found experimentally in aqueous solutions for $CH_3C(OH)OONO$ and $(CH_3)_2C(OH)OONO$.[8] The dramatic decrease in the bond strength of O–O upon replacing H by an alkyl group has been noted before for both hydroperoxides[44] and peroxynitrites.[8] This effect has been attributed to the hyperconjugative stabilization of the alkoxyl radical as opposed to that of the unstabilized $^\bullet OH$ radical.

In conclusion, the reaction of $ROO^\bullet$ with $^\bullet NO_2$ forms relatively long-lived alkyl peroxynitrates, which are in equilibrium with the parent molecules and show no tendency to homolyze along the O–O bond. In contrast, the reaction of $ROO^\bullet$ with $^\bullet NO$ forms relatively short-lived alkyl peroxynitrites, which homolyze quickly along the O–O bond.

References and Notes

(1) Rubbo, H.; Radi, R.; Trujillo, M.; Telleri, R.; Kalyanaraman, B.; Barnes, S.; Kirk, M.; Freeman, B. A. *J. Biol. Chem.* **1994**, *269*, 26066–26075.

(2) O'Donnell, V. B.; Chumley, P. H.; Hogg, N.; Bloodsworth, A.; DarleyUsmar, V. M.; Freeman, B. A. *Biochemistry* **1997**, *36*, 15216–15223.

(3) Hogg, N.; Kalyanaraman, B. *Biochim. Biophys. Acta* **1999**, *1411*, 378–384.

(4) Rubbo, H.; Radi, R.; Anselmi, D.; Kirk, M.; Barnes, S.; Butler, J.; Eiserich, J. P.; Freeman, B. A. *J. Biol. Chem.* **2000**, *275*, 10812–10818.

(5) Kotamraju, S.; Hogg, N.; Joseph, J.; Keefer, L. K.; Kalyanaraman, B. *J. Biol. Chem.* **2001**, *276*, 17316–17323.

(6) O'Donnell, V. B.; Freeman, B. A. *Circ. Res.* **2001**, *88*, 12–21.

Reaction of Peroxyl Radicals with •NO₂ and •NO

J. Phys. Chem. A, Vol. 108, No. 10, 2004 **1725**

(7) Padmaja, S.; Huie, R. E. *Biochem. Biophys. Res. Commun.* **1993**, *195*, 539−544.

(8) Merenyi, G.; Lind, J.; Goldstein, S. *J. Am. Chem. Soc.* **2002**, *124*, 40−48.

(9) Logager, T.; Sehested, K. *J. Phys. Chem.* **1993**, *97*, 6664−6669.

(10) Neta, P.; Dizdaroglu, M.; Simic, M. G. *Isr. J. Chem.* **1984**, *24*, 25−28.

(11) Erben-Russ, M.; Michel, C.; Bors, W.; Saran, M. *J. Phys. Chem.* **1987**, *91*, 2362−2365.

(12) Avila, D. V.; Brown, C. E.; Ingold, K. U.; Lusztyk, J. *J. Am. Chem. Soc.* **1993**, *115*, 466−470.

(13) Gilbert, B. C.; Holmes, R. G. G.; Laue, H. A. H.; Norman, R. O. C. *J. Chem. Soc., Perkin Trans. 2* **1976**, 1047−1052.

(14) Konya, K. G.; Paul, T.; Lin, S. Q.; Lusztyk, J.; Ingold, K. U. *J. Am. Chem. Soc.* **2000**, *122*, 7518−7527.

(15) Ilan, Y.; Rabani, J.; Henglein, A. *J. Phys. Chem.* **1976**, *80*, 1558−1562.

(16) Bothe, E.; Schultefrohlinde, D.; Sonntag, C. V. *J. Chem. Soc., Perkin Trans. 2* **1978**, 416−420.

(17) Bothe, E.; Schuchmann, M. N.; Schultefrohlinde, D.; Vonsonntag, C. *Photochem. Photobiol.* **1978**, *28*, 639−644.

(18) Logager, T.; Sehested, K. *J. Phys. Chem.* **1993**, *97*, 10047−10052.

(19) Goldstein, S.; Czapski, G. *Free Radical Biol. Med.* **1995**, *19*, 505−510.

(20) Goldstein, S.; Czapski, G. *Inorg. Chem.* **1997**, *36*, 4156−4162.

(21) Goldstein, S.; Czapski, G.; Lind, J.; Merenyi, G. *Inorg. Chem.* **1998**, *37*, 3943−3947.

(22) Schmidt, E. *Ber. Dtsch. Chem. Ges.* **1919**, *52*, 400−413.

(23) Flyunt, R.; Leitzke, A.; Mark, G.; Mvula, E.; Reisz, E.; Schick, R.; von Sonntag, C. *J. Phys. Chem. B* **2003**, *107*, 7242−7253.

(24) Mallard, W. G.; Ross, A. B.; Helman, W. P. *NIST Standard References Database 40,* version 3.0; 1998.

(25) Bielski, B. H. J.; Cabelli, D. E.; Arudi, R. L.; Ross, A. B. *J. Phys. Chem. Ref. Data* **1985**, *14*, 1041−1100.

(26) Lymar, S. V.; Schwarz, H. A.; Czapski, G. *J. Phys. Chem. A* **2002**, *106*, 7245−7250.

(27) Goldstein, S.; Czapski, G. *Free Radical Biol. Med.* **1995**, *19*, 505−510.

(28) Zegota, H.; Schuchmann, M. N.; Vonsonntag, C. *J. Phys. Chem.* **1984**, *88*, 5589−5593.

(29) Rabani, J.; Pick, M.; Simic, M. *J. Phys. Chem.* **1974**, *78*, 1049−1051.

(30) Bors, W.; Michel, C.; Saran, M. *FEBS Lett.* **1979**, *107*, 403−406.

(31) Schuchmann, M. N.; Sonntag, C. V. *J. Phys. Chem.* **1979**, *83*, 780−784.

(32) Regimbal, J. M.; Mozurkewich, M. *J. Phys. Chem. A* **1997**, *101*, 8822−8829.

(33) Kirchner, F.; Mayer-Figge, A.; Zabel, F.; Becker, K. H. *Int. J. Chem. Kinet.* **1999**, *31*, 127−144.

(34) Zabel, F.; Reimer, A.; Becker, K. H.; Fink, E. H. *J. Phys. Chem.* **1989**, *93*, 5500−5507.

(35) Bahta, A.; Simonaitis, R.; Heicklen, J. *J. Phys. Chem.* **1982**, *86*, 1849−1853.

(36) DeMore, W. B.; Sander, S. P.; Golden, D. M.; Hampson, R. F.; Kurylo, M. J.; Howard, C. J.; Ravishankara, A. R.; Molina, M. J. *Chemical Kinetics and Photochemical Data for Use in Stratospheric Modeling*; JPL: Pasadena, CA, 1992.

(37) Mayer-Figge, A.; Zabel, F.; Becker, K. H. *J. Phys. Chem.* **1996**, *100*, 6587−6593.

(38) Jonsson, M. *J. Phys. Chem.* **1996**, *100*, 6814−6818.

(39) Schwartz, S. E.; White, W. H. Kinetics of Reactive Dissolution of Nitrogen Oxides into Aqueous Solution. In *Trace Atmospheric Species: Properties, Transformations and Fates*; Schwartz, S. E., Ed.; Wiley & Sons: New York, 1983; pp 1−116.

(40) $\Delta G_f°(CH_3O•$, g) = 9.2 kcal/mol can be calculated from Berkowitz, J.; Ellison, G. B.; Gutman, F. *J. Phys. Chem.* **1994**, *98*, 2744−2765. According to Schwarz, H. A.; Dodson, R. W. *J. Phys. Chem.* **1984**, *88*, 3643−3647, the Gibbs energy of hydration, $\Delta G°_{g−aq}$, of an alcohol or a hydroperoxide is more negative by about 2 kcal/mol than that of the corresponding oxyl or peroxyl radical derived from the parent by the abstraction of a hydrogen. Because $\Delta G°_{g−aq}(CH_3OH) = −3.2$ kcal/mol (*Selected Values of Thermodynamic Properties*; U.S. Department of Commerce, National Bureau of Standards: Washington. DC, 1968; *NBS Tech. Note (U.S.)* No. 270−273) and $\Delta G°_{g−aq}(CH_3OOH)$ are about the same (O'Sullivan, D. W.; Lee, M.; Noone, B. C.; Heikes, B. G. *J. Phys. Chem.* **1996**, *100*, 3241−3247), we set $\Delta G°_{g−aq}(CH_3O•) \approx \Delta G°_{g−aq}(CH_3OO•) = −1.2$ kcal/mol. Then $\Delta G_f°(CH_3O•$, aq) $\approx 9.2−1.2 = 8.0$ kcal/mol. $\Delta G_f°(CH_3OO•$, g) ≈ 12.5 kcal/mol was calculated using $\Delta H_f°(CH_3OO•$, g) ≈ 2.8 kcal/mol (Benson, S. W.; Cohen, N. In *Peroxyl Radicals*; Alfassi, Z., Ed.; Wiley & Sons: Chichester, England, 1997; pp 49−68) and $S°$-$(CH_3OO•$, g) = 64.7 e.u (Kondo, O., Benson, W. S. *J. Phys. Chem.* **1984**, *88*, 6675−6680). Utilizing $\Delta G°_{g−aq}(CH_3OO•) = −1.2$ kcal/mol (see above), we obtained $\Delta G°_f(CH_3OO•$, aq) ≈ 11.3 kcal/mol.

(41) Stanbury, D. M. *Adv. Inorg. Chem.* **1989**, *33*, 69−138.

(42) Merenyi, G.; Lind, J.; Czapski, G.; Goldstein, S. *Inorg. Chem.* **2003**, *42*, 3796−3800.

(43) Merenyi, G.; Lind, J.; Goldstein, S. *J. Phys. Chem. A* **2002**, *106*, 11127−11129.

(44) Cremer, D. General and Theoretical Aspects of the Peroxide Group. In *The Chemistry of Peroxides*; Patai, S., Ed.; John Wiley: Chichester, England, 1983; pp 1−84.

(45) Merenyi, G.; Lind, J.; Goldstein, S.; Czapski, G. *J. Phys. Chem. A* **1999**, *103*, 5685−5691.